

Analysis of Some Optical Properties of a Native and Reconstituted Photosystem II Antenna Complex, CP29: Pigment Binding Sites Can Be Occupied by Chlorophyll *a* or Chlorophyll *b* and Determine Spectral Forms[†]

Elisabetta Giuffr ,^{‡,⊥} Giuseppe Zucchelli,^{||} Dorianna Sandon ,[‡] Roberta Croce,^{||} Daniela Cugini,[‡] Flavio M. Garlaschi,^{||} Roberto Bassi,[‡] and Robert C. Jennings^{*,||}

Centro CNR Biologia Cellulare e Molecolare delle Piante, Dipartimento di Biologia, Universit  di Milano, Via Celoria 26, 20133 Milano, Italy, and Universit  di Verona, Facolt  di Scienze MMFFNN, Biotecnologie Vegetali, Strada Le Grazie, 37134 Verona, Italy

Received May 14, 1997; Revised Manuscript Received July 28, 1997[⊗]

ABSTRACT: The minor photosystem II antenna complex CP29(Lhcb-4) has been reconstituted *in vitro* with the Lhcb-4 apoprotein, overexpressed in *Escherichia coli*, and the native pigments. Modulation of the pigment composition during reconstitution yields binding products with markedly different chlorophyll *a/b* binding ratios even though the total number of bound chlorophylls (*a* plus *b*) remains constant at eight. A thermodynamic analysis of steady state absorption and fluorescence spectra demonstrates that all chlorophylls are energetically coupled, while the kinetics of chlorophyll photooxidation indicate that triplet chlorophyll–carotenoid coupling is also conserved during pigment binding *in vitro*. The influence of the chlorophyll *a/b* binding ratio on the absorption spectra measured at 72 and 300 K is analyzed for the Q_y absorption region. Increased chlorophyll *b* binding leads to large increases in absorption in the 640–660 nm region, while absorption in the 675–690 nm interval decreases markedly. These changes are analyzed in terms of a Gaussian decomposition description in which the eight subbands display a temperature-dependent broadening in agreement with the weak electron–phonon coupling demonstrated for other antenna chlorophyll spectral forms. In this way, we demonstrate that increased chlorophyll *b* binding leads to increased absorption intensity associated with the subbands at 640, 648, 655, and 660 nm and decreased intensity for the long wavelength subbands at 678 and 684 nm. The wavelength position of all subbands is unchanged. The above data are interpreted to indicate that CP29 has eight chlorophyll binding sites, many or all of which can be occupied by either chlorophyll *a* or chlorophyll *b* according to the conditions in which pigment binding occurs. Chlorophyll *b* absorption is primarily associated with four subbands located at 640, 648, 655, and 660 nm. The invariance of the wavelength position of the absorption bands in recombinant products with different chlorophyll *a/b* binding stoichiometries is discussed in terms of the mechanism involved in the formation of spectral bands. We conclude that pigment–protein interactions dominate in the determination of spectral heterogeneity with probably only minor effects on absorption associated with pigment–pigment interactions.

Photosystems of plants are made up of a number of chlorophyll–protein complexes each of which binds many chl^I molecules. While the outer antenna complexes of PSII and PSI bind the chemically distinct chlorophylls *a* and *b*, the core complexes contain only chl *a*. A detailed understanding of energy transfer processes in the antenna and reaction centers requires knowledge of the topological organization of subunits (Bassi & Dainese, 1992; Boekema

et al., 1995) and knowledge of distances between chromophores, mutual transition dipole orientation, and absorption and fluorescence energy levels. In the case of photosystem II, progress has been made in understanding the topological organization of subunits and their spectral form composition (Hemelrijk et al., 1992; Jennings et al., 1993; Krawczyk et al., 1993; Zucchelli et al., 1994). Moreover, elucidation of the structure of the major antenna complex LHCII to a resolution of 3.7   (K hlbrandt et al., 1994) has allowed identification of chlorophyll binding sites. From this structure, it is evident that many of the binding site environments are chemically distinct and that nearest neighbor chlorophylls are spaced by 8–15  . The orientation of electronic transition dipole moments of the chromophores cannot yet be obtained from the structural data, but linear dichroism analysis suggests considerable orientation heterogeneity (Hemelrijk et al., 1992; Zucchelli et al., 1994).

It has been apparent for many years that the chlorophyll proteins are spectroscopically complex. Thus, while only one, or at the most two, chemically distinct chlorophyll species are present, depending on the complex, many optical transitions (spectral forms) are commonly observed in the

[†] This work was supported in part by the “Piano Nazionale Biotecnologie Vegetali”, MIRAAF (Italy).

^{*} To whom correspondence should be addressed E-mail: Robert.Jennings@unimi.it.

[‡] Universit  di Verona.

^{||} Universit  di Milano.

[⊥] Present address: Department of Animal Breeding and Genetics, Swedish University of Agricultural Sciences, Uppsala, Sweden.

[⊗] Abstract published in *Advance ACS Abstracts*, September 15, 1997.

¹ Abbreviations: CD, circular dichroism; chl, chlorophyll; CP, chlorophyll–protein; nCP29, native protein purified from thylakoid membranes; rCP29(*x*), recombinant protein obtained by reconstitution *in vitro* of the overexpressed apoprotein with the chromophores, with *x* referring to the chl *a/b* ratio of the reconstituted complex; DCCD, dicyclohexylcarbodiimide; FWHM, full width at half-band maximum; LHC II, light-harvesting complex of PSII; PS, photosystem.

Q_y absorption region. From this point of view, the most extensively studied complex is probably LHCII, which displays a markedly heterogeneous broadening in the 640–685 nm range. From optical spectroscopic measurements, between 8 and 11 spectral forms have been identified with reasonable certainty (Hemelrijk et al., 1992; Kwa et al., 1992; Krawczyk et al., 1993; Nussberger et al., 1994; Reddy et al., 1994; Zucchelli et al., 1996), while the number of bound chlorophylls per monomer is in the range of 12–14 (Dainese & Bassi, 1991; Kühlbrandt & Wang, 1991; Kühlbrandt et al., 1994). The physical origin of these spectral forms has been extensively discussed in recent years, though, to date, little progress has been made. A number of general possibilities exist. (1) Each spectral form is determined primarily by interactions with the pigment binding site environment. In this hypothesis, the spectral forms are essentially associated with monomer chlorophylls bound to energetically nonequivalent sites. (2) The spectral bands are primarily determined by moderate to strong Coulombic interactions between the transition dipoles of closely bound pigments. In this hypothesis, the bands are excitonically determined and are therefore not specifically associated with single binding sites [for review, see van Grondelle et al. (1994)], though different site energies may be involved in modulating the excitonic bands (Shipman et al., 1976). (3) At least some of the spectral bands are due to the coupling of electronic transitions to thermally active protein vibrational modes, possibly in the 100–150 cm^{-1} frequency range. While this suggestion (Zucchelli et al., 1996) is of particular relevance to the red-most spectral forms of the chl *a/b* complexes of PSII, it may also have important consequences for shorter wavelength bands. In this hypothesis, the vibrational components of the spectral bands are not associated with specific pigment sites and can, in principle, be derived from either monomeric or excitonically coupled transitions.

Lack of progress in developing a more detailed understanding of this spectroscopic heterogeneity has been in part due to the absence of experimental techniques making possible selective modification of the optical transitions. Thus, it has not even been possible to assign particular transitions to chl *a* or chl *b* with certainty in the chl *a/b* binding proteins, though it is generally assumed that the shorter wavelength bands are associated with chlorophyll *b* (van Metter, 1977; Hemelrijk et al., 1992). This problem becomes particularly difficult if reasonably strong Coulombic interactions between the Q_y transition dipoles of chl *a* and chl *b* occur, as has been suggested for LHCII on the basis of CD spectra (Ide et al., 1987; Hemelrijk et al., 1992).

In the context of obtaining a more detailed understanding of the chl spectral forms, the approach of pigment–protein reconstitution is particularly interesting. Experiments of this kind have been first performed using apoproteins from which pigments had been detached by detergent treatment (Plumley & Schmidt, 1987) and, more recently, by the overexpression of cDNA coding for single gene products (Paulsen et al., 1990; Cammarata & Schmidt, 1992). In most of these cases, however, the optical properties of the reconstituted complexes are somewhat different from those of the native complexes. Thus, significantly blue-shifted absorption spectra are usually reported as well as some changes in the long wavelength CD signal (Peterman et al., 1996). This clearly limits their usefulness for detailed spectroscopic studies. The successful

reconstitution of the minor chl *a/b* antenna complex, CP29, using the maize *Lhcb4* apoprotein overexpressed in *Escherichia coli*, was recently reported (Giuffra et al., 1996). This reconstituted complex has absorption, fluorescence emission, and CD spectra which closely resemble those of the native complex. The reconstituted complex also binds DCCD (Pesaresi et al., 1997) as does the native complex (Walters et al., 1994). It was furthermore demonstrated that the chl *a/b* ratio could be substantially modulated during reconstitution, yielding binding products with modified chl *a/b* content. In this paper, we present a detailed analysis of some optical properties of native and reconstituted CP29. Evidence is presented from thermal equilibrium and pigment photooxidation studies that chlorophyll and carotenoid molecules are “correctly” bound to the apoprotein. Selective chlorophyll photooxidation together with spectral decomposition analysis of complexes with modified chl *a*/chl *b* composition has allowed identification of four spectral bands associated primarily with chl *b*. This is interesting as the average number of bound chl *b* molecules per native CP29 complex is about two. Furthermore, the red-most chl *a* bands are shown to be markedly sensitive to the number of bound chl *b* molecules. These data are discussed in terms of the chl *a* and chl *b* binding sites and of the mechanisms responsible for the origin of the spectral bands. We conclude that the pigment–protein interactions in the different binding sites are of primary importance in determining spectroscopic heterogeneity, with only minor spectroscopic effects associated with chlorophyll–chlorophyll interactions.

MATERIALS AND METHODS

Construction of the CP29 (Lhcb4) Expression Plasmid. To overexpress plant CP29 in *E. coli*, the maize *Lhcb4* cDNA (Bergantino et al., 1995) was subcloned in an expression vector of the pDS series (Bujard et al., 1987) as described by Giuffra et al. (1996). The construct was checked by DNA sequencing.

Isolation of the Overexpressed CP29 Apoprotein from Bacteria. The CP29 apoprotein was isolated from the SG13009 strain transformed with the CP29 construct following published protocols (Nagai & Thogersen, 1987; Paulsen et al., 1990).

Pigments. Total pigments were extracted from thylakoids of wild-type (WT) maize with 80% acetone, while chlorophyll *a* was obtained from thylakoids of the chlorophyll *b*-less mutant *chlorina f2* (Simpson, 1979). Chlorophyll *b* and individual carotenoids were purified by preparative HPLC using a reverse phase C18 column bondclone according to Gilmore and Yamamoto (1991). Pigment concentrations were determined as described by Porra et al. (1989) for chlorophylls and by Davies (1976) for xanthophylls. The concentration of carotenoid mixtures was estimated on the basis of an average percent absorption coefficient of 2500 at 444 nm (Davies, 1976).

Reconstituted complexes and the native protein were analyzed for pigment composition after 80% acetone extraction and HPLC analysis with a Spherisorb S5 ODS1 column as previously described (Bassi et al., 1993). Care was taken to protect pigments from light and contact with oxygen.

Reconstitution and Purification of CP29–Pigment Complexes. Reconstitution and purification were performed as previously described (Giuffra et al., 1996). For stoichiometric determinations (pigment/protein ratios), it was neces-

sary to obtain a fully purified complex which did not contain any residual contamination by bacterial proteins. This was obtained by preparative IEF of the reconstituted complex (Dainese et al., 1990) followed by DEAE chromatography in order to eliminate ampholytes and glycine which would interfere with the ninhydrin reaction used to measure the protein concentration (Hirs, 1967). The concentration of the CP29 apoprotein purified from *E. coli* inclusion bodies was determined by the bicinchoninic acid assay (Smith et al., 1985).

Isolation of Native CP29. Native CP29 was isolated from maize PSII membranes as previously described (Dainese et al., 1990; Dainese & Bassi, 1991).

Spectroscopy. The absorption and the fluorescence emission spectra were measured using an EG&G OMALIII instrument (model 1460) with an intensified diode array (model 1420) mounted on a spectrograph (Jobin-Yvon HR320) with a 150 groove mm^{-1} grating as previously described (Zucchelli et al., 1996). For absorption measurements, light from a halogen lamp was used, filtered by a LP560 filter (Ditric Optics) to eliminate the blue part of the incident radiation, and attenuated by neutral filters (Balzers). Thirty thousand scans were accumulated for each spectrum. Fluorescence was excited at 440 nm, with a FWHM of 2 nm, and measured at 90 °C. For each fluorescence spectrum, about 2×10^5 counts at the maximum were accumulated. The emission spectra were corrected for instrumental response using a response function obtained measuring an intensity-calibrated source (ISCO Spectroradiometer Calibration). All samples contained 10 mM Hepes (pH 7.6) and 0.03% dodecyl maltoside.

Low-temperature absorption spectra were measured in 60% glycerol as previously described (Zucchelli et al., 1996), and residual absorption at 750 nm was subtracted.

Circular dichroism spectra were measured at 8 °C with a Jasco 600 spectropolarimeter.

Numerical decomposition of the absorption spectra has been performed as previously described (Jennings et al., 1993; Zucchelli et al., 1994), using an algorithm that minimizes the χ^2 with respect to the parameters of a model function defined as a linear combination of Gaussians. Each Gaussian function is defined as the sum of two half-Gaussians (double Gaussian). In this way, each subband has two independent band widths, right and left, and this can, in principle, describe the presence of asymmetry.

Chlorophyll Photooxidation. CP29 samples, prepared as described above for room-temperature absorption and fluorescence measurements, were illuminated at 5 °C with white light (500 W m^{-2}), obtained from a 1000 W xenon lamp filtered with a Calflex C filter (Balzers) and 4 cm of water. Absorption spectra were measured before and after various illumination times. The integrated areas of the absorption spectra in the Q_y region were used to determine the relative chlorophyll content.

RESULTS

Biochemical Characterization. Reconstitution of the CP29 apoprotein overexpressed in *E. coli* using pigment mixtures with different chlorophyll *a*/chlorophyll *b* ratios yielded chlorophyll–proteins showing absorption spectra with altered features. When a chl *a/b* ratio of 8 was used during reconstitution, a chlorophyll *a/b* binding ratio of 2.9 was

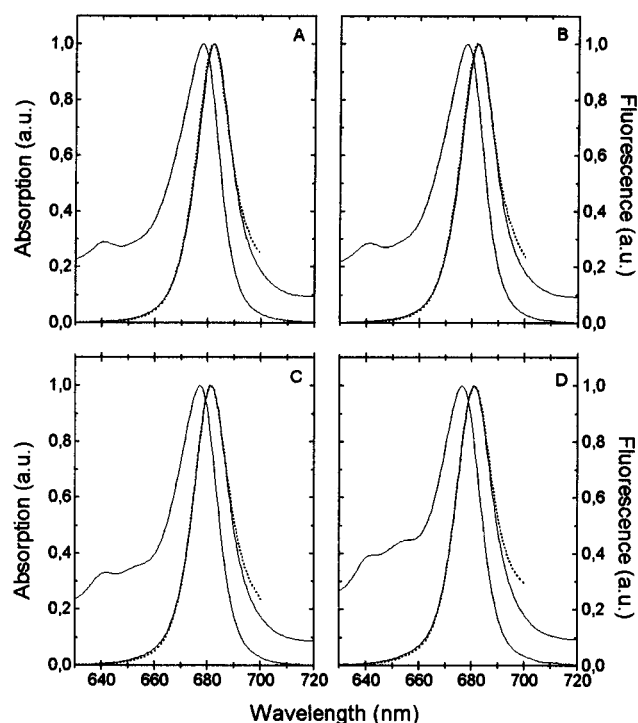


FIGURE 1: Comparison between calculated (dotted line) and measured (solid line) steady state fluorescence spectra for native and reconstituted CP29 complexes with different chl *a/b* binding ratios. Emission spectra were calculated from the absorption spectra using eq 1: (A) native CP29 with a chl *a/b* binding ratio of 2.8, (B) CP29 reconstituted with a chl *a/b* binding ratio of 2.9, (C) CP29 reconstituted with a chl *a/b* binding ratio of 2.12, and (D) CP29 reconstituted with a chl *a/b* binding ratio of 1.18.

obtained, similar to that of the native complex. The absorption spectrum also closely matched that of the native complex (Giuffra et al., 1996; Figure 1). With chl *a/b* ratios of 3, 1, and 0.1 in the reconstitution mixture, recombinant proteins with chl *a/b* ratios of 2.12, 1.18, and 0.38, respectively, were obtained. The increased chlorophyll *b* binding in these recombinant complexes is evident in the absorption spectra in the 640–665 nm region (Figure 1). In this paper, the chlorophyll–proteins analyzed will be indicated as (for native) nCP29 and (for recombinant) rCP29-(2.9), rCP29(2.12), rCP29(1.18), and rCP29(0.38) according to the increasing chl *b* content. Detailed pigment stoichiometry was performed by HPLC analysis of 80% acetone-extracted pigments (Table 1); a chlorophyll to xanthophyll ratio of 4 was obtained with both nCP29 and rCP29(2.9). Since the chlorophyll to protein stoichiometry was consistently found to be 8 in both nCP29 and rCP29(2.9), this implies that two xanthophylls are bound per CP29 polypeptide. This is in agreement with recent reports (Pesaresi et al., 1996; Croce et al., 1996), though previous studies reported somehow a lower chlorophyll to carotenoid ratio (Bassi et al., 1993; Giuffra et al., 1996), possibly indicating three xanthophyll molecules per CP29 polypeptide. This discrepancy is due to differences in pigment determination methods. We found that the efficiency of most non-encapped columns for chlorophylls and carotenoids evolves over time, thus leading to changes in the total chlorophyll to total carotenoid ratios in different determinations. Therefore, we now integrate HPLC analysis with a spectroscopic analysis which involves matching the absorption spectrum of 96% ethanol pigment extracts with composite spectra made up

Table 1: HPLC Pigment Analysis of the Native CP29 and of the Recombinant Proteins Obtained by Reconstitution of Recombinant Apoprotein with Different Pigment Mixtures^a

chl <i>a/b</i> ratio (reconstitution mixture)	neoxanthin	violaxanthin	lutein	chl <i>b</i>	chl <i>a</i>	chl <i>a/b</i> ratio	chl/xant. ratio
0.1	27.3	22.8	44.0	263.9	100	0.38	3.87
1	13.6	9.0	25.8	84.5	100	1.18	3.81
8	8.1	9.8	14.9	34.5	100	2.90	4.1
native	8.1	11.5	13.8	35.7	100	2.80	4.04

^a Pigment contents (moles) are normalized to a chl *a* value of 100 mol.

of individual purified pigments, as previously described for LHCII (Connelly et al., 1997). On the basis of the chlorophyll to xanthophyll ratio, rCP29(1.18) and rCP29-(0.38) contained an average number of 4.1 chl *a* and 3.5 chl *b* molecules and 2.1 chl *a* and 5.6 chl *b* molecules per polypeptide, respectively (Table 1).

Stepanov Analysis. In pigment–protein complexes in which both vibrational relaxation within pigment excited states and energy transfer between pigments are rapid with respect to the excited state lifetime, thermal equilibration between all intra- and intermolecular energy levels is rapidly attained. This situation is described well by the Stepanov expression (Stepanov, 1957; van Metter & Knox, 1976; Zucchelli et al., 1992), which connects the absorption and fluorescence spectra:

$$\frac{F(\nu)}{A(\nu)} = C(T) \nu^3 \exp\left(-\frac{h\nu}{kT}\right) \quad (1)$$

where $A(\nu)$ is the absorption spectrum, $F(\nu)$ is the emission spectrum, ν is the frequency, $C(T)$ is independent of frequency, k is the Boltzmann constant, T is the absolute temperature, and h is Planck's constant.

In the case of energetically uncoupled pigments which are unable to transfer excitation energy to neighboring pigments, thermal equilibration will not occur and eq 1 does not hold. As we have previously demonstrated (Zucchelli et al., 1995), the sensitivity of this approach allows the easy detection of somewhat less than one uncoupled pigment per complex (10% of the total oscillator strength), assuming that this pigment has the same fluorescence yield as the coupled pigments. As the fluorescence yield of uncoupled pigments is usually somewhat greater than that of coupled pigments, we expect this approach to be able to detect around one-half of an uncoupled pigment per complex.

In Figure 1, the Stepanov analysis is presented for nCP29 and rCP29 which had been reconstituted with different chl *a/b* binding ratios. The fluorescence spectra, calculated from the absorption spectra according to eq 1, are compared with the measured spectra. In all cases, a quite good correspondence between calculated and measured emission spectra is observed over most of the emission band. A deviation on the red side of the emission band, similar to that previously observed for the reaction center complex of PSII (Zucchelli et al., 1995), is however present. We believe this to be associated with an overestimation of the true absorption in this region due to a residual amount of light scattering and conclude that this analysis suggests rather complete thermalization in these reconstituted complexes. It therefore seems likely that chl binding occurs "correctly" in the rCP29 complexes irrespective of their chl *a*/chl *b* content.

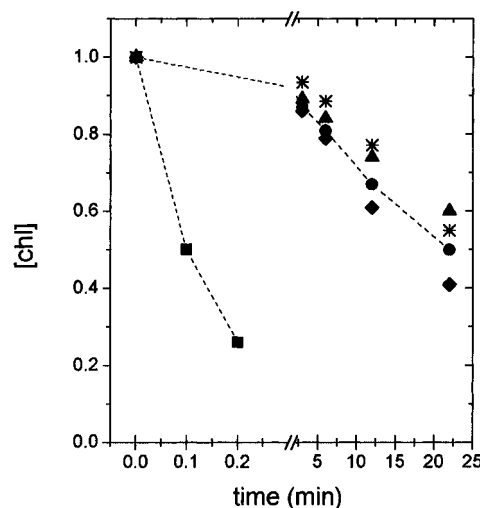


FIGURE 2: Chlorophyll photooxidation kinetics of native CP29, reconstituted CP29, and Triton X-100 (5%)-solubilized CP29: (●) native CP29 (chl *a/b* binding ratio of 2.8), (▲) reconstituted CP29 with a chl *a/b* binding ratio of 2.9, (◆) reconstituted CP29 with a chl *a/b* ratio of 2.12, (*) reconstituted CP29 with a chl *a/b* binding ratio of 1.18, and (■) Triton X-100-solubilized CP29.

Photooxidation Kinetics of Reconstituted CP29. It is well-known that carotenoids quench chl triplets and hence protect the chl–protein complexes from photooxidative damage [for review, see Siefermann-Harms (1987) and Yamamoto and Bassi (1996)]. The transfer of chl triplet excitation to car is via the so-called exchange coupling mechanism (Dexter, 1953), which requires van der Waals contact between donor and acceptor species. In order to determine whether xanthophyll binding in rCP29 is functionally correct during reconstitution, we have measured the kinetics of chlorophyll photooxidation (Figure 2). It is clear that these kinetics are rather similar in both reconstituted and the native complex, and more than 2 orders of magnitude slower than those for detergent-solubilized chlorophyll. Thus efficient chl → car triplet transfer is demonstrated, presumably indicating the correctness of pigment binding.

Selective Chl Photooxidation. The photooxidation of chl–protein complexes is partially selective for some chl absorption bands (Garlaschi et al., 1994; Jennings et al., 1994). We have therefore subjected CP29 to limited photooxidative treatments. In Figure 3A,B, the photooxidation difference spectra are presented for native CP29 and the reconstituted complex rCP29(1.18). It is evident that in both cases the chls associated with the main red absorption band, as well as the minor one near 640 nm, are particularly sensitive to photooxidation. On the other hand, absorption in the spectral region between 640 and 665 nm is markedly less sensitive. Interestingly, it is the absorption in this spectral region which increases when reconstitution is performed with high chl *b* levels, presumably indicating chl *b* absorption. This point

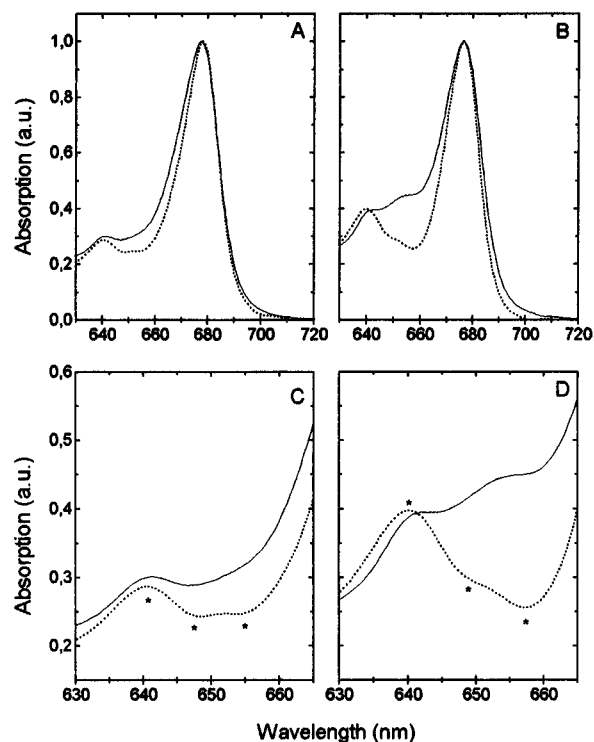


FIGURE 3: Absorption spectra (solid lines) and photooxidation difference spectra (dotted lines) of native and reconstituted CP29: (A) native CP29 and (B) reconstituted CP29 with a chl *a/b* binding ratio of 1.18. The photooxidation difference spectra have been normalized to the absorption spectra at the peak wavelength. Panels C and D show the same spectra of A and B rescaled in the wavelength range of 630–670 nm; * indicate the approximate wavelength positions of the photooxidation absorption structures.

is discussed more fully below. The similar spectral sensitivity to photooxidation of the reconstituted complexes and native complexes suggests similar binding site environments.

In Figure 3C,D, the photooxidation spectra are rescaled in the 620–670 nm interval. It is evident that in both complexes the lower sensitivity to photooxidation between 640 and 665 nm is associated with two absorption structures at approximately 648 and 655 nm. It therefore seems reasonable to conclude that these represent chl *b* absorption bands which are present in native and reconstituted complexes. The 640 nm absorption structure, clearly visible in all spectra, also appears to increase with increased chl *b* binding. Thus, we suggest at this stage that there are at least three absorption bands associated with chl *b* in CP29.

Gaussian Decomposition of Absorption Spectra. Absorption spectra in the Q_y absorption region of the native CP29 complex and some rCP29 were measured at room temperature and 71 K (Figure 4). It is evident that increased binding of chl *b* leads to a marked blue shift, which is quantitatively shown in Table 2 in terms of the mean wavelength position. This blue shifting is due to two distinct factors: increased chl *b* absorption in the blue region and a decrease in the red wing of the main (chl *a*) band. To analyze this situation more carefully, we have performed a Gaussian decomposition analysis of all spectra.

Previous Gaussian decomposition studies on native CP29 (Jennings et al., 1993; Zucchelli et al., 1994) have shown that a good description is possible with a minimum number of five subbands. This minimal description, however, proved unsatisfactory in describing the absorption spectra of complexes binding increased amounts of chl *b*. In addition, the

Table 2: Mean Wavelength Position of the Red Absorption Bands of Native and Reconstituted CP29 Complexes with Different Chl *a/b* Binding Ratios^a

	λ_{mean} (nm) ($\langle\nu\rangle$ cm ⁻¹)	
	71 K	300 K
nCP29	669.4 (14 939)	670.5 (14 914)
rCP29(2.9)	668.7 (14 954)	669.7 (14 931)
rCP29(1.18)	665.2 (15 034)	667.5 (14 982)
rCP29(0.38)	660.7 (15 136)	662.8 (15 088)

^a Values are given in both wavelength and frequency units. The moments analysis was performed between 640 and 720 nm.

band widths due to electron–phonon coupling and site inhomogeneous broadening for antenna chls in a variety of chl–protein complexes are expected to be around 9–11 nm at room temperature and 6–7 nm at 71 K (Jennings et al., 1994; Cattaneo et al., 1995; Zucchelli et al., 1996). This constraint, which was not previously considered, has been used in the present study. In this way, we have arrived at a Gaussian description with eight major, essentially symmetric, subbands between 640 and 685 nm (Table 3). It is reassuring that the band shapes come out symmetrical, even though our decomposition routine allows asymmetry, as this is expected for antenna chls at medium to high temperatures (Zucchelli et al., 1996). This description, in terms of band positions and the apparent thermal sensitivity of band widths, is very similar to that recently presented for LHCII (Zucchelli et al., 1996). It should be noted that the three short wavelength bands at 640, 648, and 655 nm are in excellent agreement with the absorption structures identified in photooxidation difference spectra (Figure 3).

As pointed out above, the total number of chl molecules bound per CP29 polypeptide in the different reconstitution conditions remained essentially constant at eight, even though the chl *a/b* binding ratio changed dramatically (Table 1). This clearly suggests that when the chl *a/b* ratio is low in the reconstitution mixture chl *b* molecules bind to protein sites which are occupied by chl *a* molecules in the native complex. However, as can be seen in Table 3, the wavelength positions of the decomposition subbands do not change significantly. Thus, it should be relatively simple to identify at least some of the bands associated with chl *b* absorption by determining those in which the absorption intensity increases with increasing chl *b* binding. In order to do this, it is necessary to normalize these spectra to some appropriate parameter. As the extinction coefficients of chls *a* and *b* are significantly different, it is not correct to normalize to the total integrated area under the Q_y absorption band. To this end, we have therefore used the measured chl *a/b* stoichiometries, assuming a relative chl *b*/chl *a* extinction ratio of 0.7, which is based on the solvent values (Sauer et al., 1966). In this way, the total measured Q_y absorption areas for the different complexes were rescaled to the calculated total chl *a* plus *b* extinction. Changes in subband intensity are presented as a function of the amount of bound chl *b* in Figure 5 for both the room temperature and 71 K spectra. It is evident that the changes in intensity for the different subbands fall into three categories. With increasing chl *b*, all four short wavelength subbands display increases in intensity, the extent of which is approximately similar except for the 640 nm band, which seems to change somewhat less. On the other

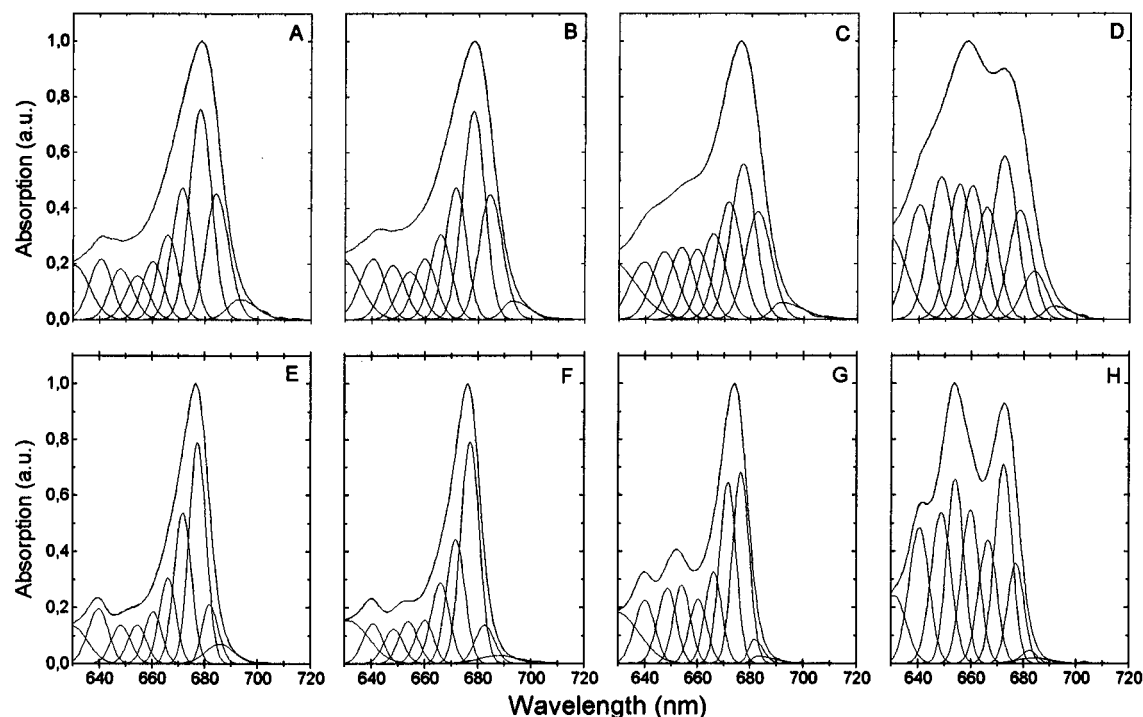


FIGURE 4: Gaussian subband analysis of absorption spectra of native and reconstituted CP29 measured at 71 and 300 K. Panels A–D depict the room-temperature spectra, while panels E–H depict the 71 K spectra: (A and E) native CP29, (B and F) reconstituted CP29 with a chl *a/b* binding ratio of 2.9, (C and G) reconstituted CP29 with a chl *a/b* binding ratio of 1.18, (D and H) reconstituted CP29 with a chl *a/b* binding ratio of 0.38. The subband parameters are shown in Table 3.

Table 3: Gaussian Decomposition Parameters for Native and Reconstituted CP29 Complexes with Different Chl *a/b* Binding Ratios^a

nCP29			rCP29(2.9)			rCP29(1.18)			rCP29(0.38)		
λ_{\max} (nm)	area (%)	FWHM (cm ⁻¹)	λ_{\max} (nm)	area (%)	FWHM (cm ⁻¹)	λ_{\max} (nm)	area (%)	FWHM (cm ⁻¹)	λ_{\max} (nm)	area (%)	FWHM (cm ⁻¹)
<i>T</i> = 300 K											
641	7.9	249 ± 6	641	8.6	272.4	640	8.3	293 ± 9	641	12.3	
648.5	6.8	255 ± 5	648	7.2	251.5	648	9.5	270 ± 14	649	15	255 ± 16
655	5.8	243 ± 5	655	6.5	252.9	654.5	9.4	242 ± 20	656	13.6	237 ± 12
661	7.1	212 ± 2	660.5	7.6	228.5	660	8.8	233 ± 15	660.5	13.7	240 ± 7
666.5	10.1	201 ± 10	666.5	9.9	207.7	666.5	11	234 ± 15	666	11.2	228 ± 8
672	15.6	200 ± 8	672	15.3	203.7	672	15.3	229 ± 19	672.5	16.9	232 ± 8
678.5	26.8	206 ± 6	678.5	25.8	212.8	677.5	20.2	223 ± 22	678.5	10.9	222 ± 7
684.5	16.6		684.5	16.3		683	14.7		684	5	
693.5	3.4		693	2.7		692	2.8		691.5	1.4	
<i>T</i> = 71 K											
640	8.8	224 ± 2	641	6.6	210	640.5	10.1	228 ± 8	641	14	
649	5.9	206 ± 3	649	5.7	205.6	649	11.1	195 ± 2.3	649	15.5	217 ± 8
655	5.5	191 ± 1	654.5	6.8	197.8	654.5	10.6	184 ± 5.5	654.5	16.1	185 ± 8
661	7.2	178 ± 3	660.5	6.6	182.8	661	8.8	183 ± 7.2	660.5	14.3	194 ± 10
666.5	11	167 ± 1	666.5	12.5	184.8	667	12	177 ± 11	667	11.5	189 ± 10
672	20.6	171 ± 2	672	18.9	178.7	672	23.4	171 ± 8	673	17.9	181 ± 11
677.5	29.5	166 ± 3	677.5	34	176.7	677	25	170 ± 8	677.5	8.5	172 ± 12
682	7.7		683	6.3		682	2.8		682.5	1.1	
686	3.9		689	2.7		683	1.4		685.5	1	

^a The data are graphically represented in Figure 4 and refer to measurements performed at 300 and 71 K.

hand, the red-most bands show a very marked decline in intensity with increased chl *b* binding, whereas the 666 and 672 nm bands change very little.

The large decrease in the 684 nm and minor longer wavelength subbands at low temperatures has been previously noted for all chl *a/b* proteins of PSII and extensively studied in LHCII (Zucchelli et al., 1990, 1994, 1996).

CD Spectra. The CD spectra for the various analyzed CP29 complexes are presented in Figure 6. The general structure in both the Soret and red regions is similar to that previously reported for the native complex (Giuffrè et al., 1996). In the red region, the CD signal almost completely

spans the absorption band and is strongly nonconservative. In this spectral region, a progressive blue shifting of the main negative lobe occurs on lowering the chl *a/b* binding ratio. This is dramatic in the rCP29(0.38) complex, where the 680 nm band is replaced by a broad, obviously composite structure between 660 and 670 nm. Comparison with the absorption changes (Figures 1, 4, and 5) suggests that the blue shifting in CD is associated with the drastic decrease in the long wavelength absorption bands at low chl *a/b* binding ratios together with an increase in the CD signal at wavelengths described by the 666 and 672 nm absorption bands.

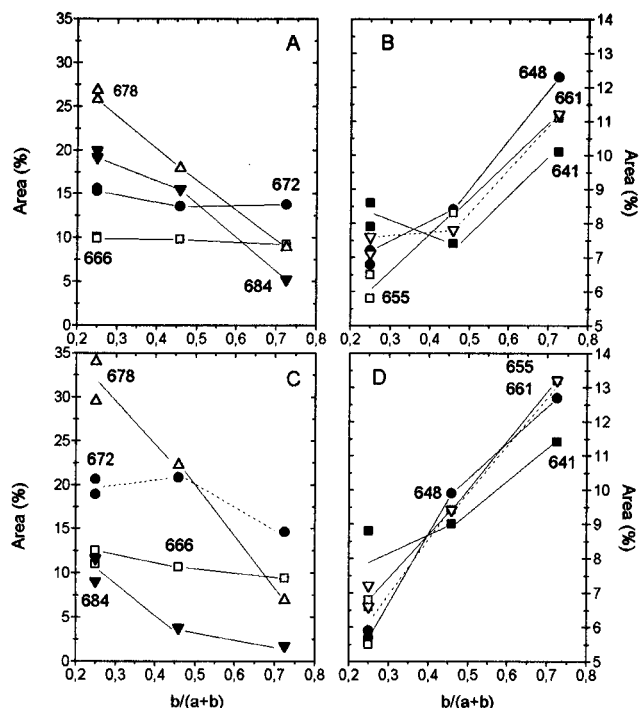


FIGURE 5: Changes in Gaussian subband area as a function of bound chl *b* in CP29 complexes. The data points refer to the recombinant complexes with chl *a/b* binding ratios of 0.38, 1.18, and 2.9 and the native complex with a chl *a/b* binding ratio of 2.8. Normalization of the different spectra was performed as described in the text using the relative, solvent, extinction values for a chl *b*/chl *a* ratio of 0.7/1.0. Panels A and B refer to the room-temperature analysis. Panels C and D refer to the 71 K analysis. The numbers indicate the wavelength position of the Gaussian subbands.

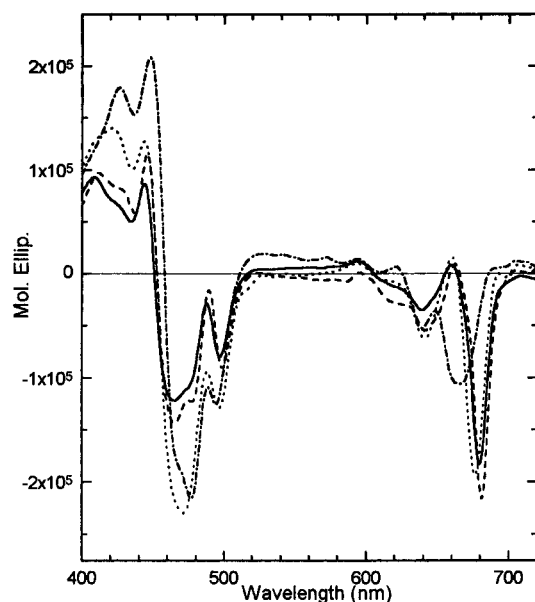


FIGURE 6: Circular dichroism spectra for native and reconstituted CP29 complexes: native CP29 (solid line) and rCP29 with chl *a/b* binding ratios of 2.9 (dashed line), 1.18 (dotted line), and 0.38 (dashed-dotted line). Spectra were normalized to the same total chl *a* plus chl *b* concentration as determined by HPLC analysis.

DISCUSSION

In this paper, data are presented on some biochemical and optical properties of native CP29 and CP29 produced from recombinant proteins reconstituted with different chl *a/b* ratios. Pigment stoichiometry analysis indicates that while the bound chl *a/b* ratio changes drastically the total number

of bound chls remains at about eight. This suggests that CP29 has eight chl binding sites which may be occupied by either chl *a* or chl *b*. This point is further developed below.

In order for the reconstituted complexes to be "spectroscopically useful", it is necessary to demonstrate that pigment binding occurs in a specific and correct way and that the complex is functionally competent. To this end, we performed two distinct kinds of experiments. In the first place, the absorption/fluorescence relationship was analyzed with the Stepanov expression (eq 1). This analysis demonstrated that thermal equilibration is essentially attained in both native and reconstituted complexes, thus showing that all pigments are coupled energetically. In the second kind of experiment, chl photooxidation kinetics were measured in the reconstituted complexes and demonstrated to be similar to those of the native complex. This indicates that the strict structural requirements for ^3chl to ^1car transfer, via the electron exchange mechanism of Dexter (1953), are maintained. Furthermore, the chl *b* molecules absorbing between 640 and 665 nm are similarly sensitive to photo-oxidation in the native and reconstituted complexes. These observations, together with the similarity of rCP29(2.9) and the native complex in some optical properties, strongly indicate that pigment binding occurred correctly during the present reconstitution experiments. To our knowledge, similarly successful reconstitution has not been previously reported for chl-protein complexes.

In the remaining discussion, we will address the relevance of the present experiments to an understanding of the absorption bands (spectral forms) in chlorophyll *a/b* proteins. In order to accurately describe both room-temperature and 71 K absorption in the 640–665 nm region, taking into account reasonable values for the inhomogeneously broadened band widths (9–11 nm at room temperature and 6–7 nm at 71 K), four Gaussian subbands are required, with wavelength positions at 640, 648, 655, and 660 nm. The 640 nm band is obviously associated with the secondary absorption peak near this wavelength. Independent evidence for the 648 and 655 nm transitions comes from photooxidation experiments where absorption structures are evident in the difference spectra. When increasing amounts of chl *b* were bound during reconstitution, all four subbands increase in intensity, while other subbands either remain approximately constant or decrease. Thus, it is clear that these four subbands are associated with chl *b* absorption. An interesting point which should be emphasized is that we are unable to detect significant changes in the wavelength positions of these four chl *b* transitions by either Gaussian analysis or photooxidation difference spectra, even though the average binding stoichiometry for chl *b* changes from about two to six molecules per polypeptide. Thus, it seems that the number of spectral bands associated with chl *b* in the native complex as well as in rCP29(2.9) is greater than the average number of bound chl *b* molecules. This clearly indicates chl *b* binding heterogeneity at the level of the different complexes. We therefore envisage each CP29 preparation as representing a mixed site population of bound chl *b* molecules. This suggestion is in line with the conclusion, discussed above, that most chl binding sites may bind either chl *a* or chl *b*. Some of these binding sites appear to be energetically degenerate, as in rCP29(0.38), binding an average of six chl *b* molecules, the four chl *b* absorption forms are not significantly altered. The exact population

binding ratio is expected to be determined at least in part by the chl *a/b* ratio present during pigment–protein folding both *in vivo* and *in vitro*. This is in agreement with previous work on plants grown in intermittent light in which a lower chl *b* availability caused a higher chlorophyll *a/b* ratio in CP29 and CP26 proteins (Marquardt & Bassi, 1993). The fact that 666 and 672 nm absorption forms are much less sensitive to chl *b* binding than the longer wavelength chl *a* forms may indicate that chl sites have different chl *a*/chl *b* binding affinities.

We will now attempt to evaluate the relative importance of site energies or pigment–pigment interactions in determining the absorption bands of CP29. The prominent CD signals, which are sensitive to the chl *a/b* binding ratio, may indicate the presence of excitonic interactions between pigments [e.g. van Metter (1977), Braun et al. (1990), and Hemelrijk et al. (1992)]. We start out by considering whether chl *b*–chl *b* interactions may be of significant importance, as has been suggested for LHCII (van Metter, 1977; Gulen & Knox, 1984). For simplicity, only excitonically coupled dimers will be considered, though we realize that, in chl–protein complexes, Coulombic interactions may occur between a number of pigment sites. We have checked whether the general conclusions which come out of the simplified “dimer type” approach are significantly modified in a “multimer-type” situation by analyzing eight site quadratic interaction energy (*J*) matrices (Shipman et al., 1976): $J_{ij} = 5.04k(\mu_i\mu_j/R^3)$, where μ is the monomer transition moment (Debyes), *k* is a dipole orientation term, and *R* is the *i*–*j* center to center distance. These calculations show that the dimer type approach provides a good description, to a first approximation, of the energy spread of excitonic bands. We therefore prefer to use the simple dimer approach in the absence of precise crystallographic structural data. As discussed above, four chl *b* subbands are present at apparently the same wavelength positions irrespective of the average number of bound chl *b* molecules per complex. These bands span a 20 nm (500 cm^{−1}) interval and are separated by about 6–8 nm. Thus, in order to provide an explanation in substantially excitonic terms (similar site energies), it is necessary to assume rather high values for the chl *b*–chl *b* matrix interaction energies (*J* = 80–250 cm^{−1}). If we take a solvent Q_y dipole strength for chl *b* of 15 D² and assume a perfect “head to tail” transition dipole orientation, this *J* value interval requires that the center–center distances be extremely short (0.85–1.2 nm). These values are in the lower range of the nearest neighbor distances determined by Kühlbrandt and Wang (1991) and Kühlbrandt et al. (1994) for LHCII and are thus presumably near the upper limit for chl *b*–chl *b* interaction energies. While it is not difficult to imagine a number of strong chl *b*–chl *b* interactions in the reconstituted complexes with low chl *a/b* binding ratios, this is not possible in the case of complexes binding an average of two chl *b* molecules per polypeptide, distributed over different binding sites. We therefore conclude that chl *b*–chl *b* interactions are unlikely to be particularly important in determining the wavelength positions of the four chl *b* subbands. In support of this conclusion is the apparently invariant wavelength position of these subbands as the number of bound chl *b* molecules goes from two to six per complex.

We now address the subject of spectroscopically significant chl *a*–chl *a* and chl *a*–chl *b* interactions. We will take the

approach of attempting to explain our observations in terms of pigment–pigment “excitonic” interactions. The data show that as chl *b* binds in place of chl *a* there is a marked decline in the intensity of the long wavelength chl *a* absorption subbands ($\lambda \geq 678$ nm) while the shorter wavelength chl *a* bands remain substantially unchanged in both intensity and wavelength position. In the excitonic interaction hypothesis, this observation can be readily interpreted in terms of the red-most bands representing the low-energy transition of excitonic chl *a* dimers. As about 65% of the total chl *a* oscillator strength is in these long wavelength transitions, interactions would presumably be between substantially head to tail-oriented dipoles (Cantor & Schimmel, 1980). Interaction between head to tail-oriented dipoles not only gives rise to the low-energy transition possessing most of the intensity but also is favorable for high *J* values. When chl *b* occupies the binding site of one of an interacting chl *a* pair in CP29 complexes with low chl *a/b* binding ratios, the chl *a*–chl *a* interaction will be broken and replaced by a chl *a*–chl *b* interaction. In this case, however, the excitonic bands associated with the chl *a*–chl *b* interactions will be rather close to the noninteracting monomer absorption positions, even if the *J* values are rather high, due to the substantially nonresonant transition energies of the chl *a* and chl *b* monomers [see eq 20 in Shipman et al. (1976)]. To illustrate this point more clearly, we give a simple numerical example. Let us assume that the 678 nm chl *a* subband is the low-energy excitonic transition of two interacting chl *a* molecules with monomer absorption at 672 nm. Thus, *J* = 130 cm^{−1}. When this chl *a*–chl *a* interaction is replaced by a chl *a*–chl *b* interaction, and assuming no change in dipole orientation, the *J* value decreases slightly to 110 cm^{−1} due to the weaker chl *b* transition moment. However, owing to the approximately 500 cm^{−1} (20 nm) difference in monomer transition energies, the excitonic effects on spectral shifting are greatly reduced and pass from 6 nm in the case of the resonant chl *a*–chl *a* interaction to 1 nm in the case of the nonresonant chl *a*–chl *b* interaction. This could in principle explain the marked decrease in the red-most bands with increasing chl *b* binding. The 666 and 672 nm bands, associated here with chl *a*, could thus represent the low-energy bands of chl *a*–chl *b* excitonic dimers and monomeric chl *a* absorption in the excitonic interaction hypothesis. However, in this explanation for rCP29(0.38), one expects chl *b*–chl *b* interactions to replace the chl *a*–chl *a* interactions present in the complexes with high chl *a/b* binding ratios. In the case of the above numerical example in which *J* = 130 cm^{−1} for chl *a*–chl *a* interactions (a minimum value to explain the red bands in terms of excitonic band shifts), the *J* value for chl *b*–chl *b* interactions is expected to be around 90 cm^{−1} if dipole orientations for chl *b* are similar to those for chl *a* at the same binding site. It is clear that such a relatively strong interaction would give rise to easily detectable spectral shifts associated with the establishment of these chl *b*–chl *b* interactions. However, as discussed above, no change in the chl *b* band positions are detected with changing chl *a/b* binding stoichiometries. This comment is particularly applicable to the shortest wavelength subband (640 nm). From our dimer-type and quadratic *J* matrix-type calculations, it is evident that the wavelength position of this band is particularly sensitive to changes in the chl–chl interactions. As this band is associated with a very clear absorption structure at all chl *a/b* binding ratios,

it is easily defined by spectral decomposition. We are therefore forced to conclude that it is difficult to interpret either the chl *a* or chl *b* subbands in terms of significant shifts in the monomer absorption transitions due to excitonic interactions. Site energies thus seem to play a dominant role in determining the absorption energies, and the long wavelength chl *a* sites seem to be readily occupied by chl *b*.

We now briefly discuss the CD spectra which display strong, nonconservative signals across the Q_y region and which undergo marked blue shifting as the chl *a/b* binding ratio decreases. If these signals are in fact due to chl–chl interactions, as is usually assumed [however, see Büchel and Garab (1997)] from the above discussion, we conclude that these interactions must be quite weak. In order to explain the apparent constancy of the chl *b* subband positions, we feel that the matrix energies for chl *b*–chl *b* interactions should not exceed 20–30 cm^{−1} and thus be no more than 30–45 cm^{−1} for chl *a*–chl *a* interactions. Such low *J* values, while having only slight effects on the absorption bands which we may be unable to detect, can give rise to strong CD signals depending on dipole orientation and interchromophore distances (Cantor & Schimmel, 1980). The loss of the strong negative CD lobe near 680 nm, which is replaced by signals in the 666–672 nm region in complexes with low chl *a/b* binding ratios, clearly correlates with the absorption changes.

Finally, we comment on the longest wavelength subbands ($\lambda_{\max} \geq 684$ nm). These bands display a marked temperature sensitivity (Figures 4 and 5) as has already been extensively documented for similar bands in LHCII (Zucchelli et al., 1990, 1996). This temperature sensitivity cannot be readily explained in terms of either site-dependent energies or excitonic interactions. We therefore suggest, as shown previously for LHCII, that the red-most subbands may be associated with coupling to thermally active protein vibrations. In this case, the 684 nm band represents a Q_y(1,0) transition of the Q_y(0,0) positioned at 678 nm, with coupling to a vibrational frequency ν of ≈ 130 cm^{−1}.

These results may be summarized as follows. By using recombinant proteins with altered chlorophyll *a/b* compositions, we show that eight chl binding sites are present on CP29. Four chl *b* absorption forms are identified between 640 and 661 nm which are apparently invariant in wavelength position as the average number of chl *b* molecules per complex changes from two to six. The data are interpreted as indicating that most chl sites can bind either chl *a* or chl *b*. The invariant wavelength position of chl *a* and chl *b* absorption bands with changing chl *a/chl b* binding stoichiometries suggests that excitonic interactions are not important in determining the spectroscopic characteristics of the chlorophyll forms. We therefore conclude that pigment–protein interactions are mainly responsible for spectral heterogeneity.

REFERENCES

- Bassi, R., & Dainese, P. (1992) *Eur. J. Biochem.* 204, 317–326.
- Bassi, R., Pineau, B., Dainese, P., & Marquardt, J. (1993) *Eur. J. Biochem.* 212, 297–303.
- Bergantino, E., Dainese, P., Cerovic, Z., Sechi, S., & Bassi, R. (1995) *J. Biol. Chem.* 270, 8474–8481.
- Boekema, E. J., Hankamer, B., Bald, D., Kruip, J., Nield, J., Boonstra, A. F., Barber, J., & Rogner, M. (1995) *Proc. Natl. Acad. Sci. U.S.A.* 92, 175–179.
- Braun, P., Greenberg, B. M., & Scherz, A. (1990) *Biochemistry* 29, 10376–10387.
- Büchel, C., & Garab, G. (1997) *J. Photochem. Photobiol., B* 37, 118–124.
- Bujard, H., Gentz, R., Lanzer, M., Stueber, D., Mueller, M., Ibrahim, I., Haeuptle, M. T., & Dobberstein, B. (1987) in *Methods in Enzymology Recombinant DNA. Part C* (Wu, R., Ed.) Vol. 155, pp 416–433, Academic Press, New York.
- Cammarata, K. V., & Schmidt, G. W. (1992) *Biochemistry* 31, 2779–2789.
- Cantor, C. R., & Schimmel, P. R. (1980) *Biophysical Chemistry*, W. H. Freeman and Co., San Francisco.
- Cattaneo, R., Zucchelli, G., Garlaschi, F. M., Finzi, L., & Jennings, R. C. (1995) *Biochemistry* 34, 15267–15275.
- Connelly, J. P., Müller, M. G., Bassi, R., Croce, R., & Holzwarth, A. R. (1997) *Biochemistry* 36, 281–287.
- Dainese, P., & Bassi, R. (1991) *J. Biol. Chem.* 266, 8136–8142.
- Dainese, P., Hoyer-Hansen, G., & Bassi, R. (1990) *Photochem. Photobiol.* 51, 693–703.
- Davies, B. H. (1976) in *Chemistry and Biochemistry of Plant Pigments* (Goodwin, T. W., Ed.) 2nd ed., Vol. 2, Chapter 19, pp 38–165, Academic Press, New York.
- Dexter, D. L. (1953) *J. Chem. Phys.* 21, 836–850.
- Garlaschi, F. M., Zucchelli, G., Giavazzi, P., & Jennings, R. C. (1994) *Photosynth. Res.* 41, 465–473.
- Gilmore, A. M., & Yamamoto, H. Y. (1991) *J. Chromatogr.* 543, 137–145.
- Giuffra, E., Cugini, D., Croce, R., & Bassi, R. (1996) *Eur. J. Biochem.* 238, 112–120.
- Gulen, D., & Knox, R. S. (1984) *Photobiochem. Photobiophys.* 7, 277–286.
- Hemelrijk, P. W., Kwa, S. L. S., van Grondelle, R., & Dekker, J. P. (1992) *Biochim. Biophys. Acta* 1098, 159–166.
- Hirs, C. H. W. (1967) in *Methods in Enzymology* (Hirs, C. H. W., Ed.) Vol. 11, pp 325–329, Academic Press, New York.
- Ide, J. P., Klug, D. R., Kühlbrandt, W., Giorgi, L. B., & Porter, G. (1987) *Biochim. Biophys. Acta* 893, 349–364.
- Jennings, R. C., Bassi, R., Garlaschi, F. M., Dainese, P., & Zucchelli, G. (1993) *Biochemistry* 32, 3203–3210.
- Jennings, R. C., Garlaschi, F. M., Finzi, L., & Zucchelli, G. (1994) *Liet. Fiz. Rinkiny* 34, 293–300.
- Krawczyk, S., Krupa, Z., & Maksymiec, W. (1993) *Biochim. Biophys. Acta* 1143, 273–281.
- Kühlbrandt, W., & Wang, D. N. (1991) *Nature* 350, 130–134.
- Kühlbrandt, W., Wang, D. N., & Fujiyoshi, Y. (1994) *Nature* 367, 614–621.
- Kwa, S. L. S., Groeneveld, F. G., Dekker, J. P., van Grondelle, R., van Amerongen, H., Lin, S., & Struve, W. S. (1992) *Biochim. Biophys. Acta* 1101, 143–146.
- Marquardt, J., & Bassi, R. (1993) *Planta* 191, 265–273.
- Nagai, K., & Thogersen, H. C. (1987) in *Methods in Enzymology, Recombinant DNA. Part D* (Wu, R., & Grossman, L., Eds.) Vol. 153, pp 461–481, Academic Press, New York.
- Nussberger, S., Dekker, J. P., Kühlbrandt, W., Vanbolhuis, B. M., Vangrondelle, R., & Vanamerongen, H. (1994) *Biochemistry* 33, 14775–14783.
- Paulsen, H., Rumler, U., & Rudiger, W. (1990) *Planta* 181, 204–211.
- Pesaresi, P., Sandona, D., Giuffra, E., & Bassi, R. (1997) *FEBS Lett.* 402, 151–156.
- Peterman, E. J. G., Hobe, S., Calkoen, F., van Grondelle, R., Paulsen, H., & van Amerongen, H. (1996) *Biochim. Biophys. Acta* 1273, 171–174.
- Plumley, F. G., & Schmidt, G. W. (1987) *Proc. Natl. Acad. Sci. U.S.A.* 84, 146–150.
- Porra, R. J., Thompson, W. A., & Kriedermann, P. E. (1989) *Biochim. Biophys. Acta* 975, 384–394.
- Reddy, N. R. S., van Amerongen, H., Kwa, S. L. S., van Grondelle, R., & Small, G. J. (1994) *J. Phys. Chem.* 98, 4729–4735.
- Sauer, K., Lindsay-Smith, J. R., & Schulz, A. J. (1966) *J. Am. Chem. Soc.* 88, 2681–2688.
- Shipman, L. L., Norris, J. R., & Katz, J. J. (1976) *J. Phys. Chem.* 80, 877–882.
- Siefermann-Harms, D. (1987) *Physiol. Plant.* 69, 561–568.
- Simpson, D. J. (1979) *Carlsberg Res. Commun.* 44, 305–336.

- Smith, K., Krohn, R. I., Hermanson, G. T., Mallia, A. K., Gartner, F. H., Provenzano, O., Fujimoto, E. K., Goeke, N. M., Olsen, B. J., & Klenk, D. C. (1985) *Anal. Biochem.* 150, 76–85.
- Stepanov, B. I. (1957) *Sov. Phys. Dokl.* 2, 81–84.
- van Grondelle, R., Dekker, J. P., Gillbro, T., & Sundstrom, V. (1994) *Biochim. Biophys. Acta* 1187, 1–65.
- van Metter, R. L. (1977) *Biochim. Biophys. Acta* 462, 642–658.
- van Metter, R. L., & Knox, R. S. (1976) *Chem. Phys.* 12, 333–340.
- Walters, R. G., Ruban, A. V., & Horton, P. (1994) *Eur. J. Biochem.* 226, 1063–1069.
- Yamamoto, H., & Bassi, R. (1996) in *Oxygenic Photosynthesis: The Light Reactions* (Ort, D. R., & Yokum, C. F., Eds.) pp 539–563, Kluwer Academic Publishers, Dordrecht, The Netherlands.
- Zucchelli, G., Jennings, R. C., & Garlaschi, F. M. (1990) *J. Photochem. Photobiol., B* 6, 381–394.
- Zucchelli, G., Jennings, R. C., & Garlaschi, F. M. (1992) *Biochim. Biophys. Acta* 1099, 163–169.
- Zucchelli, G., Dainese, P., Jennings, R. C., Breton, J., Garlaschi, F. M., & Bassi, R. (1994) *Biochemistry* 33, 8982–8990.
- Zucchelli, G., Garlaschi, F. M., Croce, R., Bassi, R., & Jennings, R. C. (1995) *Biochim. Biophys. Acta* 1229, 59–63.
- Zucchelli, G., Garlaschi, F. M., & Jennings, R. C. (1996) *Biochemistry* 35, 16247–16254.

BI9711339